

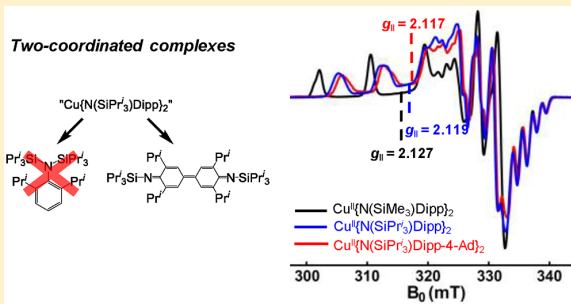
## Two-Coordinate, Late First-Row Transition Metal Amido Derivatives of the Bulky Ligand $-\text{N}(\text{SiPr}^i_3)\text{Dipp}$ (Dipp = 2,6-diisopropylphenyl): Effects of the Ligand on the Stability of Two-Coordinate Copper(II) Complexes

Clifton L. Wagner, Lizhi Tao,<sup>1</sup> James C. Fettinger,<sup>1</sup> R. David Britt,<sup>1</sup> and Philip P. Power\*<sup>1,2</sup>

Chemistry Department, University of California, Davis, One Shields Avenue, Davis, California 95616, United States

### Supporting Information

**ABSTRACT:** The synthesis and spectroscopic, structural, and magnetic characterization of the quasi-linear metal(II) bis(amides)  $\text{M}\{\text{N}(\text{SiPr}^i_3)\text{Dipp}\}_2$  [Dipp =  $\text{C}_6\text{H}_3\text{-}2,6\text{-Pr}^i_3$ ; M = Fe (1), Co (2), or Zn (3)] are described. The magnetic data demonstrate the impact of metal ligand  $\pi$ -interactions on the magnetic properties of these two-coordinate transition metal amides. Disproportionation of the copper(I) amide species featuring the ligand  $-\text{N}(\text{SiPr}^i_3)\text{Dipp}$  resulted in the decomposition product  $[(\text{Pr}^i_3\text{Si})\text{N}(\text{c-C}_6\text{H}_2\text{-}2,6\text{-Pr}^i_3)]_2$  (4). The electron paramagnetic resonance spectrum of the unstable two-coordinate  $\text{Cu}\{\text{N}(\text{SiPr}^i_3)\text{Dipp}\}_2$  displays significantly less Cu–N bond covalency than the stable two-coordinate copper(II) species  $\text{Cu}\{\text{N}(\text{SiMe}_3)\text{Dipp}\}_2$ . The testing of  $-\text{N}(\text{SiPr}^i_3)\text{Dipp}$  and a range of other, related bulky amide ligands with their copper derivatives highlights the peculiar combination of steric and electronic properties of the Wigley ligand  $-\text{N}(\text{SiMe}_3)\text{Dipp}$  that enable it to stabilize the unique two-coordinate copper(II) complex  $\text{Cu}\{\text{N}(\text{SiMe}_3)\text{Dipp}\}_2$ .



### INTRODUCTION

Our current understanding of the behavior and electronic properties of transition metal complexes highlights the importance of the ligand environment in determining the coordination number of the metal.<sup>1</sup> Open-shell ( $d^1\text{--}d^9$ ), two-coordinate complexes remain, with rare exception,<sup>2</sup> poorly explored due to their relative scarcity. Nonetheless, two-coordinate transition metal complexes are attracting an increased level of interest due to their relatively open, extremely reactive metal centers as well as their unique magnetic and electronic properties.<sup>2a,b,3</sup>

Recent developments in the field of open-shell two-coordinate transition metal complexes have resulted in the synthesis of a range of such derivatives using alkyl, amido, oxo, aryl, and carbene ligands.<sup>4</sup> The currently available data (ca. 160 complexes) demonstrate that only the use of the most sterically hindered of ligands can stabilize two-coordinate geometry. Exploration of different ligand sets has shown the dramatic effects of not only the first but also the second ligand sphere on the electronic properties of the two-coordinate species.<sup>2g</sup> For example, two stable bisamides of nickel, the purple  $\text{Ni}\{\text{N}(\text{SiMe}_3)\text{Dipp}\}_2$ <sup>5</sup> and the green  $\text{Ni}\{\text{N}(\text{H})\text{Ar}^{\text{Pr}^i_6}\}_2$ <sup>4d</sup> (Dipp = 2,6-diisopropylphenyl, and  $\text{Ar}^{\text{Pr}^i_6} = 2,6\text{-bis}(2,4,6\text{-triisopropylphenyl})\text{phenyl}$ ), both feature linear two-coordinate metals; however, the former has a d–d absorption at 508 nm

(19700  $\text{cm}^{-1}$ ), while the latter has a d–d absorption at 778 nm (12900  $\text{cm}^{-1}$ ), a difference of 6800  $\text{cm}^{-1}$  (19.4 kcal mol<sup>−1</sup>). This highlights the importance of the ligand composition for the electronic properties of two-coordinate transition metal complexes.

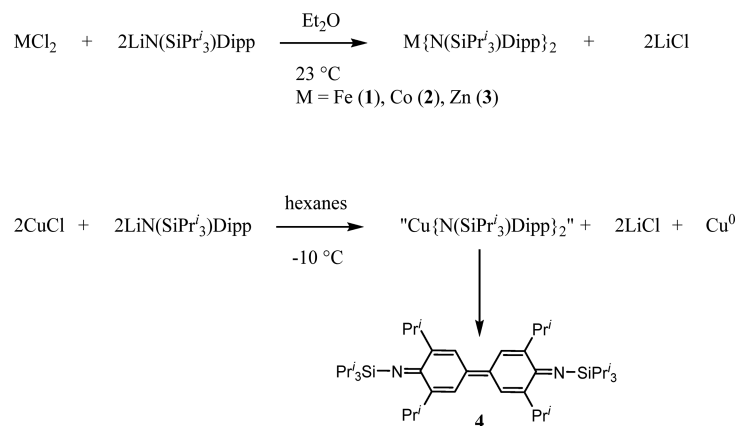
Another challenge in the chemistry of two-coordinate complexes is that the achievement of strictly linear coordination that can have a large effect on magnetic properties, for example, in the linear complexes  $\text{M}\{\text{C}(\text{SiMe}_3)_3\}_2$  (M = Mn or Fe),<sup>4a,b</sup>  $\text{M}\{\text{N}(\text{H})\text{Ar}^{\text{Pr}^i_6}\}_2$  (M = Fe, Co, or Ni),<sup>4c,d</sup> and  $\text{M}\{\text{N}(\text{SiMe}_3)\text{Dipp}\}_2$  (M = Mn, Fe, Co, or Ni)<sup>5,6</sup> whose orbital magnetic moments are mostly unquenched and where London dispersion forces (LDF) may play a role in setting the geometries.<sup>7</sup>

The latter series is particularly noteworthy because it includes the only currently known, stable two-coordinate copper(II) complex where it is believed London dispersion forces are key to its stability.<sup>6c</sup> We therefore turned to a bulkier version of the so-called Wigley ligand  $-\text{N}(\text{SiMe}_3)\text{Dipp}$  in which the  $-\text{SiMe}_3$  substituent is replaced by the bulkier  $-\text{SiPr}^i_3$  group to afford the  $-\text{N}(\text{SiPr}^i_3)\text{Dipp}$  ligand that was first reported by Luo and co-workers.<sup>8</sup> Several other ligands  $[-\text{N}(\text{SiMe}_3)_2$ ,

Received: April 23, 2019

Published: June 12, 2019

Scheme 1. Synthesis of Compounds 1–4



-N(SiPh<sub>2</sub>Me)<sub>2</sub>, -C(SiMe<sub>3</sub>)<sub>3</sub>, -OAr<sup>Ad<sub>2</sub>Me</sup>, -N(H)Ar<sup>Pr<sup>i</sup></sup>, -N(3,5-Xyl)Ad, and -N(SiMe<sub>3</sub>)Ad] (Ad = adamantyl; Ar<sup>Ad<sub>2</sub>Me</sup> = 2,6-diadamantyl-4-methylphenyl) were also tested with copper, but only -N(SiPr<sup>i</sup>)Dipp and -N(SiPr<sup>i</sup>)Dipp-4-Ad afforded signals consistent with the formation of their two-coordinate copper(II) complexes in solution.

Herein, we report the isolation and characterization of the quasi-linear two-coordinate compounds Fe{N(SiPr<sup>i</sup>)Dipp}<sub>2</sub> (**1**), Co{N(SiPr<sup>i</sup>)Dipp}<sub>2</sub> (**2**), and Zn{N(SiPr<sup>i</sup>)Dipp}<sub>2</sub> (**3**). We also report the electron paramagnetic resonance (EPR) characterization of the transient two-coordinate copper(II) species of the homoleptic species Cu{N(SiPr<sup>i</sup>)Dipp}<sub>2</sub> and Cu{N(SiPr<sup>i</sup>)Dipp-4-Ad}<sub>2</sub> (Dipp-4-Ad = 2,6-diisopropyl-4-adamantylphenyl).

## RESULTS AND DISCUSSION

Complexes **1**–**3** were synthesized by the addition of a solution of the lithium salt LiN(SiPr<sup>i</sup>)Dipp<sup>8</sup> in diethyl ether to the corresponding anhydrous metal dichloride (Scheme 1). The reaction mixtures for the formation of **1** and **3** were filtered, and the volume was decreased to ca. 15 mL. The reaction flasks were stored in a -30 °C freezer overnight to afford red and colorless crystals for Fe and Zn, respectively. The reaction mixture to form **2** did not crystallize with diethyl ether, hexanes, or pentane as the solvent. However, extraction of the reaction mixture with toluene, decreasing the solvent volume, and subsequent storage in an approximately -30 °C freezer for 1 week yielded **2** as dark brown crystals.

Similarly, the preparation of the Ni(II) variants of **1**–**3** via the reaction of 2 equiv of LiN(SiPr<sup>i</sup>)Dipp with NiCl<sub>2</sub> or NiBr<sub>2</sub> afforded elimination of the lithium halide salt and a purple-colored solution (cf. refs 2d and 5). However, workup in the usual way and attempted recrystallization from the solvents hexane, toluene, diethyl ether, tetrahydrofuran (THF), dimethyl sulfide, and hexamethyl disiloxane did not afford a crystalline product.

The addition of a solution of the lithium salt LiN(SiPr<sup>i</sup>)Dipp in hexanes to CuCl was carried out with cooling in a CaCl<sub>2</sub>/ice bath at ca. -10 °C. After 2 h at ca. -10 °C, copper metal precipitated from the reaction mixture and it became blue in color. This behavior is broadly similar to that seen for the two-coordinate copper(II) complex Cu{N(SiMe<sub>3</sub>)Dipp}<sub>2</sub><sup>6c</sup> that was sufficiently stable to isolate.

The X-ray data show that **1** has a two-coordinate quasi-linear geometry at the metal with a N–Fe–N angle of 175.86(6)° (see Figure 1). This is in contrast to the closely related bulky

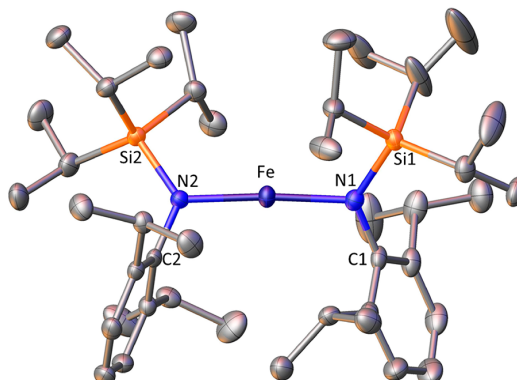
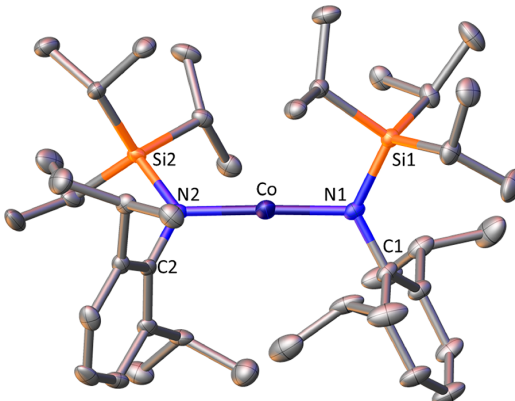


Figure 1. Molecular structure of Fe{N(SiPr<sup>i</sup>)Dipp}<sub>2</sub> (**1**). H atoms are not shown. The thermal ellipsoids are shown at the 30% probability level. Selected bond lengths (angstroms) and angles (degrees): Fe–N1, 1.8854(14); Fe–N2, 1.8911(15); N1–Si1, 1.7411(16); N2–Si2, 1.7466(15); N1–Fe–N2, 175.86(6); C1–N1–Si1, 127.54(11); C2–N2–Si2, 124.46(11).

silylamido Fe(II) species Fe{N(SiMe<sub>3</sub>)Dipp}<sub>2</sub><sup>5</sup> that has a rigorously linear N–Fe–N angle of 180.0°. The triisopropylsilyl substituent of the ligands in complex **1** adds additional steric crowding that likely prevents the eclipsed arrangement of the ligands found in Fe{N(SiMe<sub>3</sub>)Dipp}<sub>2</sub><sup>5</sup>. Instead of the eclipsed ligand orientation, complex **1** possesses a torsion angle of 44.090(3)° between the N1 and N2 coordination planes of the ligands. Calculations for the electronic structure of the two-coordinate transition metal complexes with the ligand -N(SiMe<sub>3</sub>)Dipp indicate a significant contribution from the M–N π-bonding state<sup>2d</sup> as well as the N–Si π-antibonding hyperconjugative interaction with the metal.<sup>6c</sup> This deviation from the eclipsed arrangement with a high-potential steric clash significantly disrupts M–N multiple bonding and hyperconjugation to the N–Si bond. Fe{N(SiMe<sub>3</sub>)Dipp}<sub>2</sub> has an M–N bond length (1.8532(13) Å) shorter than that in **1**, which has an average M–N bond length of 1.889(2) Å,

possibly as a result of the diminished M–N multiple-bond character.

Complex **2** also has a two-coordinate quasi-linear geometry at the metal atom with an N–M–N angle of  $175.21(10)^\circ$  (see Figure 2). The structure of **2**, like that of **1**, has a large ligand



**Figure 2.** Molecular structure of  $\text{Co}\{\text{N}(\text{SiPr}_3^i)\text{Dipp}\}_2$  (**2**). The thermal ellipsoids are shown at the 30% probability level. Only one of the two molecules in the asymmetric unit is shown. Selected bond lengths (angstroms) and angles (degrees): Co–N1, 1.859(2); Co–N2, 1.836(2); N1–Si1, 1.746(2); N2–Si2, 1.748(2); N1–Co–N2, 175.21(10); C1–N1–Si1, 123.3(2); C2–N2–Si2, 122.6(2).

torsion angle of  $41.4(8)^\circ$  between the nitrogen coordination planes.  $\text{Co}\{\text{N}(\text{SiPr}_3^i)\text{Dipp}\}_2$  is isostructural to the iron analogue and has structural details similar to those previously mentioned for iron complex **1**. While the M–N distance (average of  $1.844(5)$  Å) in **2** is significantly longer than that of  $\text{Co}\{\text{N}(\text{SiMe}_3)\text{Dipp}\}_2$  ( $1.8179(14)$  Å) it is similar to those of  $\text{Co}\{\text{N}(\text{H})\text{Ar}^{\text{Pr}_6^i}\}_2$  ( $1.8645(19)$  Å), although the ligands in both compounds possess an eclipsed arrangement of their ligand coordination planes (see Table 3).

The M–N bond lengths for the zinc species **3** (average of  $1.834(3)$  Å) fall within the known range of Zn(II)–N bond lengths in two-coordinate zinc amides (see Figure 3).<sup>2i</sup> The near linearity in the N–Zn–N bond angle resembles the linearity or near linearity generally observed in two-coordinate zinc amides (cf. Table 1). The long N–Si distances (average of  $1.746(2)$  Å) are likely due to the steric repulsion within the ligand.

The electronic spectra of **1** and **2** are very similar to those of  $\text{Fe}\{\text{N}(\text{SiMe}_3)\text{Dipp}\}_2$  and  $\text{Co}\{\text{N}(\text{SiMe}_3)\text{Dipp}\}_2$ , respectively. The iron amide electronic spectrum in hexanes has absorptions at 360 and 480 nm, while the cobalt amide has absorptions at 440 nm with a shoulder near 580 nm. While their electronic spectra may not distinguish **1** and **2** from  $\text{Fe}\{\text{N}(\text{SiMe}_3)\text{Dipp}\}_2$  (360 nm) and  $\text{Co}\{\text{N}(\text{SiMe}_3)\text{Dipp}\}_2$  (430 nm), the magnetic data are diagnostic.

The magnetic susceptibilities of **1** and **2** from 2 to 300 K were collected using a SQUID magnetometer (see the Supporting Information). The air and water sensitivity of the samples required that they be sealed in quartz tubes under vacuum. Due to the poor thermal conductivity of the sample containers, extremely long delays were necessary to reach thermal equilibrium during the initial cooling to 2 K (6 h) and at low temperatures (<10 K, 2 h).

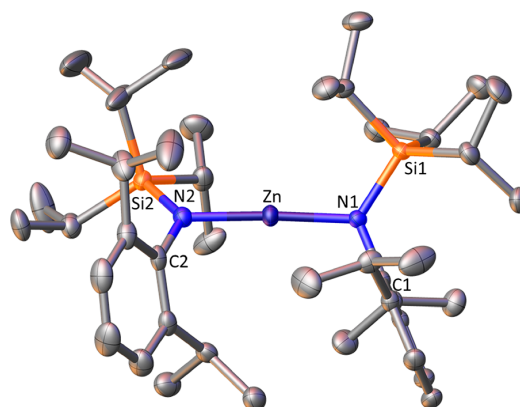


**Figure 3.** Molecular structure of  $\text{Zn}\{\text{N}(\text{SiPr}_3^i)\text{Dipp}\}_2$  (**3**). The thermal ellipsoids are shown at the 30% probability level. Only one of the two molecules in the asymmetric unit is shown. Selected bond lengths (angstroms) and angles (degrees): Zn–N1, 1.8275(14); Zn–N2, 1.8289(14); N1–Si1, 1.7415(15); N2–Si2, 1.7459(15); N1–N2–Si2, 178.04(6); C1–N1–Si1, 124.69(15); C2–N2–Si2, 123.29(14).

The magnetic data for **1** are in agreement with those for most two-coordinate iron(II) complexes (see Table 2).<sup>2g,15</sup> There is a large orbital contribution to the magnetic moment (cf.  $5.59 \mu_B$  at 110 K, which is larger than the spin only value of  $4.90 \mu_B$ ).<sup>1a</sup> However, it is not as high as the magnetic moment in the rigorously linear iron bis(amide) ( $6.04 \mu_B^S$  for  $\text{Fe}\{\text{N}(\text{SiMe}_3)\text{Dipp}\}_2$ ) or  $6.6 \mu_B$ <sup>16</sup> for the bis(alkyl)  $\text{Fe}(\text{C}(\text{SiMe}_3)_3)_2$ .

The magnetic data for the cobalt species **2** show that it has a room-temperature value of  $\sim 4.8 \mu_B$ , which is significantly greater than the calculated spin only value of  $3.87 \mu_B$ . However, the  $\mu_{\text{eff}}$  value is markedly lower than the value of  $5.93 \mu_B$  in the rigorously linear complex  $\text{Co}\{\text{N}(\text{SiMe}_3)\text{Dipp}\}_2$  (cf. the free  $\text{Co}^{2+}$  ion value of  $6.63 \mu_B$ ).<sup>1a</sup> It is closer to the  $\mu_{\text{eff}}$  values seen in the more strongly bent  $\text{Co}\{\text{N}(\text{SiMePh}_2)_2\}_2$ <sup>4g</sup> or  $\text{Co}\{\text{N}(\text{H})\text{Ar}^{\text{Me}}_6\}_2$ <sup>4d</sup> (see Table 3). Thus, the value for **2** is a notable reduction in the magnetic moment where both the first ligand sphere and the second ligand sphere are similar but the L–M–L bond angle deviates from linearity by  $<5^\circ$ . Previous isolobal ligand systems for two-coordinate structures have seen significant decreases in the magnetic moment with bending of the L–M–L angle.<sup>4d</sup> Gao and co-workers reported an apparent relationship between the ligand torsion angle and magnetic susceptibility in a series of two-coordinate iron and cobalt compounds with a heteroleptic (amide and carbene) ligand environment.<sup>17</sup> The interligand torsion angle for **2** is  $41.4(8)^\circ$ , whereas the other linear coordinated amides of cobalt have no torsion angles between ligand planes (see Table 3). Similarly, for **1**, the interligand torsion angle is  $44.090(3)^\circ$  and most of the other linear metal amides feature no ligand torsion angles between the ligand coordination (see Table 2). However, the quasi-linear  $\text{Fe}\{\text{N}(\text{SiMePh}_2)_2$  has a ligand torsion angle of  $76.64(6)^\circ$  and a corresponding magnetic moment of  $5.07 \mu_B$ .<sup>4g</sup> These examples suggest that torsion angles between the ligands and the resulting  $\pi$ -overlap<sup>2d,5,17,18</sup> have a correlation with the orbital enhancement of the magnetic moment.

Table 1. Comparison of the Structures of Two-Coordinate Zinc Silylamides

metal complex	average M–N (Å)	average N–Si (Å)	average N–C (Å)	∠N–M–N (deg)	∠L–L (deg)
3	1.8282(14)	1.7437(15)	1.443(2)	178.04(6)	43.0(5)
Zn{N(SiMe <sub>3</sub> )Dipp} <sub>2</sub> <sup>6d</sup>	1.8209(13)	1.7281(14)	1.434(2)	180	0
Zn{N(SiMe <sub>3</sub> ) <i>p</i> -2,6-Xyl} <sub>2</sub> <sup>6d</sup>	1.817(2)	1.722(3)	1.424(4)	180	19.65(11)
Zn{N(SiMe <sub>3</sub> ) <i>p</i> -C <sub>6</sub> H <sub>3</sub> -2,5-Bu <sup>t</sup> } <sub>2</sub> <sup>6d</sup>	1.838(3)	1.731(3)	1.443(4)	179.58(17)	16.67(19)
Zn{N(SiMe <sub>3</sub> ) <sub>2</sub> } <sub>2</sub>	1.824(14), <sup>a</sup> 1.833(11) <sup>b</sup>	1.729(7) <sup>b</sup>		180, <sup>a</sup> 175.2(4) <sup>b</sup>	75.43(9) <sup>b</sup>

<sup>a</sup>Structure determined by gas electron diffraction.<sup>9</sup> <sup>b</sup>Structure determined by single-crystal X-ray diffraction.<sup>10</sup>

Table 2. Comparison of M–N Distances, N–Fe–N Bond Angles, and  $\mu_{\text{eff}}$  Values for Two-Coordinate Fe(II) Amides

	M–N (Å)	∠M–N–M (deg)	$\mu_{\text{eff}}$ ( $\mu_{\text{B}}$ )
1	1.89106(11)	175.864(10)	5.59
Fe{N(SiMe <sub>3</sub> )Dipp} <sub>2</sub> <sup>5</sup>	1.8532(13)	180	5.89
Fe{N(SiMePh <sub>2</sub> ) <sub>2</sub> } <sup>11</sup>	1.901(3)	169.0(1)	5.07
Fe{N(H)Ar <sup>p<i>t</i></sup> } <sub>2</sub> <sup>8g</sup>	1.9018(17)	180	5.80
Fe{1,8-Ph <sub>2</sub> -3,6-Me <sub>2</sub> C <sub>12</sub> H <sub>4</sub> N} <sub>2</sub> <sup>12</sup>	1.9715(18)	177.92(9)	4.73
Fe{N(CH <sub>2</sub> Bu <sup>t</sup> )Dipp} <sub>2</sub> <sup>13</sup>	1.842(2)	168.8(2)	5.21
Fe{NBu <sup>t</sup> } <sub>2</sub> <sup>14</sup>	1.880(2)	179.45(8)	5.55

Table 3. Comparison of M–N Distances, N–Co–N Bond Angles, and  $\mu_{\text{eff}}$  Values for Two-Coordinate Co(II) Amides

	M–N (Å)	∠N–M–N (deg)	$\mu_{\text{eff}}$ ( $\mu_{\text{B}}$ )
2	1.844(5)	175.21(10)	4.8
Co{N(SiMe <sub>3</sub> )Dipp} <sub>2</sub> <sup>5</sup>	1.8179(14)	180	5.93
Co{N(SiMePh <sub>2</sub> ) <sub>2</sub> } <sup>11</sup>	1.901(3)	147.0	4.42
Co{N(H)Ar <sup>p<i>t</i></sup> } <sub>2</sub> <sup>19</sup>	1.8645(19)	180	6.2
Co{N(H)Ar <sup>M<sub>2</sub></sup> } <sub>2</sub> <sup>19</sup>	1.836(8)	144.1(4)	4.65
Co{N(BMes <sub>2</sub> )Mes} <sub>2</sub> <sup>4e</sup>	1.910(3)	168.4(1)	4.36
Co{N(BMes <sub>2</sub> )Ph} <sub>2</sub> <sup>4e</sup>	1.909(5)	127.1(2)	4.11

## COPPER

Many research groups have found that sterically hindered ligands promote reduction of copper(II) species to copper(I) species due, it is thought,<sup>20</sup> to the sterically crowded metal center preventing square-planar coordination that stabilizes copper(II) species. Therefore, the reported synthesis of a stable two-coordinate Cu(II) complex, Cu{N(SiMe<sub>3</sub>)Dipp}<sub>2</sub>, via copper(I) chloride was surprising, particularly due to the general stability of two-coordinate copper(I) compounds. However, this compound can be readily decomposed, in the presence of electron-rich solvents, to copper metal as well as DippNNDipp and N(SiMe<sub>3</sub>)<sub>2</sub>Dipp, the latter involving a silyl group transfer.<sup>6c</sup> To hinder this decomposition, the ligand *N*(SiPr<sub>3</sub>)Dipp was chosen with the assumption that the greater steric congestion in the *N*(SiPr<sub>3</sub>)Dipp moiety might hinder this process and enhance the stability of the metal complex. Attempts to synthesize the copper(II) analogues of **1–3** via our previously reported<sup>6c</sup> route were unsuccessful in isolating Cu{N(SiPr<sub>3</sub>)<sub>2</sub>Dipp}<sub>2</sub>, although Cu{N(SiPr<sub>3</sub>)<sub>2</sub>Dipp}<sub>2</sub> was formed as indicated by the observation of a characteristic blue color as well as an EPR spectrum (see Figure 4). It decomposes in a hexanes/pentane solution to copper metal and **4** (Scheme 1) at approximately  $-10$  °C. Although this reactivity contrasts that of V{N(SiPr<sub>3</sub>)Dipp}<sub>2</sub>,<sup>21</sup> which undergoes methyl C–H activation, it resembles that of Cu{N(SiMe<sub>3</sub>)<sub>2</sub>Dipp}<sub>2</sub> in that it appears to be accelerated by the presence of electron-rich solvents (toluene, benzene, diethyl

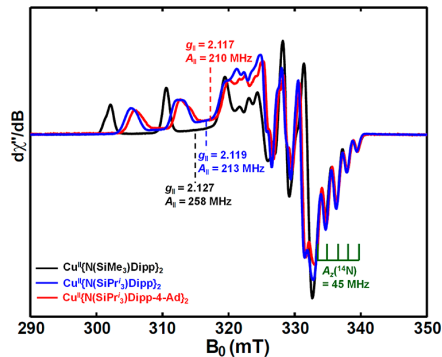


Figure 4. X-Band CW EPR spectra of a frozen solution of Cu{N(SiMe<sub>3</sub>)Dipp}<sub>2</sub> (black trace), Cu{N(SiPr<sub>3</sub>)<sub>2</sub>Dipp}<sub>2</sub> (blue trace), and Cu{N(SiPr<sub>3</sub>)Dipp-4-Ad}<sub>2</sub> (red trace) in hexanes ( $\sim 2$  mM) acquired at 30 K using a 0.063 mW power (no saturation), with the corresponding *g* tensors determined to be  $\mathbf{g} = [2.1270, 2.0425, 2.0076]$ ,  $\mathbf{g} = [2.1190, 2.0463, 2.0065]$ , and  $\mathbf{g} = [2.1170, 2.0463, 2.0065]$ , respectively. The other spectrometer settings are a microwave frequency of 9.38 GHz, a conversion time of 40 ms, a modulation amplitude of 0.3 mT, and a modulation frequency of 100 kHz.

ether, and tetrahydrofuran). A similar reactivity was encountered earlier in copper arylnitrene chemistry<sup>22</sup> and has been utilized in organic synthesis.<sup>23</sup> We have observed the same product **4** from the reaction of the lithium salt LiN(SiPr<sub>3</sub>)Dipp with either PdI<sub>2</sub> or AgCl. However, in the case of copper, the transient metal species was stable enough for EPR analysis. Additionally, reactions with the ligands LiN(SiMe<sub>3</sub>)<sub>2</sub>, LiN(SiMePh<sub>2</sub>)<sub>2</sub>, and [(THF)<sub>4</sub>Li][Li{C(SiMe<sub>3</sub>)<sub>3</sub>}<sub>2</sub>] were also attempted under the same reaction conditions but resulted only in their known copper(I) products.<sup>20g,24</sup>

The corresponding X-band (9.38 GHz) continuous-wave (CW) EPR spectrum of a frozen solution of Cu{N(SiPr<sub>3</sub>)<sub>2</sub>Dipp}<sub>2</sub> in hexanes ( $\sim 2$  mM) is shown in Figure 4 (blue trace), which resembles our previously reported spectrum of Cu{N(SiMe<sub>3</sub>)Dipp}<sub>2</sub> (Figure 4, black trace) by showing a rhombic *g* tensor and a similar superhyperfine coupling pattern from two equivalent <sup>14</sup>N nuclei ( $I = 1$ ).<sup>6c</sup> However, we observed that the  $g_{\parallel}$  ( $g_{\parallel}$ ) value of 2.119 and the <sup>63</sup>Cu hyperfine value of 213 MHz for Cu{N(SiPr<sub>3</sub>)<sub>2</sub>Dipp}<sub>2</sub> are somewhat smaller than the corresponding values for Cu{N(SiMe<sub>3</sub>)Dipp}<sub>2</sub> [ $g_{\parallel} = 2.127$ , and  $A_{\parallel}$  (<sup>63</sup>Cu) = 258 MHz], suggesting that less spin density resides on the metal Cu<sup>II</sup> center for Cu{N(SiPr<sub>3</sub>)<sub>2</sub>Dipp}<sub>2</sub> that could result from a lower Cu<sup>II</sup>–<sup>14</sup>N bond covalency.

The observation of reductive coupling through the *para* position of the aryl rings within the ligand suggested that steric hindrance of the *para* position could prevent decomposition of the transient species. Therefore, the ligand salt LiN(SiPr<sub>3</sub>)<sub>2</sub>

Dipp-4-Ad (Dipp-4-Ad = 2,6-diisopropyl-4-adamantylphenyl) was also synthesized<sup>2e,25</sup> (see the Supporting Information) and reacted with CuCl. Although the disproportionation of the Cu(I) species occurred at a slightly elevated temperature (40 °C), the disproportionation produced Cu(II){N(SiPr<sup>i</sup>)Dipp-4-Ad}<sub>2</sub>, which could not be isolated as a crystalline solid. However, as in the previous case, its EPR spectrum was observable, as shown in Figure 4 (red trace), which resembles the spectrum of Cu{N(SiPr<sup>i</sup>)<sub>2</sub>Dipp}<sub>2</sub>. The slightly smaller  $g_{\parallel}$  value of 2.117 and the <sup>63</sup>Cu hyperfine value of 210 MHz, in comparison to the parameters of Cu{N(SiPr<sup>i</sup>)<sub>2</sub>Dipp}<sub>2</sub>, suggest that the Cu<sup>II</sup> center of Cu{N(SiPr<sup>i</sup>)Dipp-4-Ad}<sub>2</sub> has a spin density comparable to but slightly lower than that of Cu<sup>II</sup> in Cu{N(SiPr<sup>i</sup>)<sub>2</sub>Dipp}<sub>2</sub>.

## CONCLUSIONS

The synthesis and magnetic properties for the quasi-linear compounds Fe{N(SiPr<sup>i</sup>)Dipp}<sub>2</sub> (1) and Co{N(SiPr<sup>i</sup>)Dipp}<sub>2</sub> (2) with use of the Luo ligand -N(SiPr<sup>i</sup>)Dipp demonstrate that, in addition to a quasi-linear geometry and the ligand coordination sphere, the potential  $\pi$ -overlap for metal amido complexes can affect their magnetic properties. The use of this more crowded ligand in the preparation of a copper(II) amide demonstrates a new decomposition pathway for the copper(II) amide. However, neither the N(SiPr<sup>i</sup>)Dipp ligand nor the N(SiPr<sup>i</sup>)Dipp-4-Ad ligand provides the required environment to stabilize the copper(II) amide. The EPR spectrum of Cu{N(SiPr<sup>i</sup>)Dipp}<sub>2</sub> suggests lower Cu–N bond covalency in this complex in comparison to that of Cu{N(SiMe<sub>3</sub>)Dipp}<sub>2</sub>.

## EXPERIMENTAL SECTION

All manipulations were performed with the use of modified Schlenk techniques or in a Vacuum Atmospheres OMNI-Lab drybox. All solvents were dried over an alumina column, followed by storage over a potassium mirror, and were degassed (freeze–pump–thaw method) prior to use. FeCl<sub>2</sub>, CoCl<sub>2</sub>, and ZnCl<sub>2</sub> were freshly dried under vacuum while being heated to 300 °C for 8 h. LiN(SiPr<sup>i</sup>)Dipp<sup>2e</sup> was synthesized according to literature procedures. Ultraviolet–visible spectra were recorded for samples as dilute hexane solutions in a 3.5 mL quartz cuvette with an Olym spectrophotometer. Melting points were measured in glass capillaries sealed under N<sub>2</sub> by using a Mel-Temp II apparatus and are uncorrected.

**Fe{N(SiPr<sup>i</sup>)Dipp}<sub>2</sub> (1).** LiN(SiPr<sup>i</sup>)Dipp (1.0 g, 3.0 mmol) was dissolved in 40 mL of Et<sub>2</sub>O and added dropwise to a suspension of freshly dried FeCl<sub>2</sub> (0.192 g, 1.5 mmol) in Et<sub>2</sub>O (10 mL). After the dark brown mixture was stirred for 24 h, it was filtered and concentrated to incipient crystallization. Storage of this mixture at approximately –30 °C overnight afforded large, orange crystals of 1 that were suitable for X-ray crystallography: yield 0.286 g (27%); mp 154 °C; UV–vis (hexane)  $\lambda_{\text{max}}$  ( $\epsilon$ ) 360 nm (1900 cm<sup>−1</sup> M<sup>−1</sup>), 465 nm (700 cm<sup>−1</sup> M<sup>−1</sup>); IR (nujol)  $\nu$  415, 440, 480, 520, 780, 880, 890, 995, 1100, 1170, 1230, 1250, 1370, 1450 cm<sup>−1</sup>.

**Co{N(SiPr<sup>i</sup>)Dipp}<sub>2</sub> (2).** LiN(SiPr<sup>i</sup>)Dipp (1.0 g, 3.0 mmol) was dissolved in 40 mL of Et<sub>2</sub>O and added dropwise to a suspension of freshly dried CoCl<sub>2</sub> (0.192 g, 1.5 mmol) in Et<sub>2</sub>O (10 mL). After the dark brown mixture was stirred for 24 h, it was filtered and the volatile materials were removed under vacuum. The residue was extracted with toluene (20 mL), and the brown filtrate was concentrated to ca. 5 mL. Storage of this mixture at ca. –30 °C overnight afforded large, brown crystals of 2 that were suitable for X-ray crystallography: yield 0.420 g (39%); mp 152 °C; UV–vis (hexane)  $\lambda_{\text{max}}$  ( $\epsilon$ ) 430 nm (3100 cm<sup>−1</sup> M<sup>−1</sup>); IR (nujol)  $\nu$  440, 490, 530, 700, 730, 780, 820, 975, 995, 1010, 1100, 1180, 1235, 1260, 1300, 1380, 1420, 1510 cm<sup>−1</sup>.

**Zn{N(SiPr<sup>i</sup>)Dipp}<sub>2</sub> (3).** LiN(SiPr<sup>i</sup>)Dipp (1.0 g, 3.0 mmol) was dissolved in 40 mL of Et<sub>2</sub>O and added dropwise to a suspension of ZnCl<sub>2</sub> (0.192 g, 1.5 mmol) in Et<sub>2</sub>O (10 mL). After the colorless

mixture was stirred for 24 h, it was filtered and concentrated to incipient crystallization. Storage of this mixture at –30 °C overnight afforded large, colorless crystals of 3 that were suitable for X-ray crystallography: yield 0.881 g (82%); mp 148 °C; IR (nujol)  $\nu$  360, 420, 440, 495, 535, 700, 740, 780, 850, 870, 900, 980, 1040, 1060, 1100, 1175, 1230, 1250, 1300, 1350, 1375, 1420, 1460 cm<sup>−1</sup>.

**EPR Spectroscopy.** The frozen solution samples for three copper compounds (~2 mM) were prepared in a nitrogen-filled glovebox by using a deoxygenated and water-free hexane solvent. The X-band (9.38 GHz) CW EPR spectra were recorded on a Bruker (Billerica, MA) Biospin EleXsys E500 spectrometer equipped with a superhigh Q resonator (ER4122SHQE). Cryogenic temperatures were achieved and controlled using an ESR900 liquid helium cryostat in conjunction with a temperature controller (Oxford Instruments ITC503) and gas flow controller. CW EPR data were collected under slow-passage, nonsaturating conditions. The spectrometer settings were as follows: conversion time of 40 ms, modulation amplitude of 0.3 mT, and modulation frequency of 100 kHz.

## ASSOCIATED CONTENT

### Supporting Information

The Supporting Information is available free of charge on the ACS Publications website at DOI: 10.1021/acs.inorg-chem.9b01159.

Further synthetic details, crystallographic parameters, electronic spectra, and <sup>1</sup>H NMR spectra (PDF)

### Accession Codes

CCDC 1906096–1906100 contain the supplementary crystallographic data for this paper. These data can be obtained free of charge via [www.ccdc.cam.ac.uk/data\\_request/cif](http://www.ccdc.cam.ac.uk/data_request/cif), or by emailing [data\\_request@ccdc.cam.ac.uk](mailto: data_request@ccdc.cam.ac.uk), or by contacting The Cambridge Crystallographic Data Centre, 12 Union Road, Cambridge CB2 1EZ, UK; fax: +44 1223 336033.

## AUTHOR INFORMATION

### Corresponding Author

\*E-mail: [pppower@ucdavis.edu](mailto: pppower@ucdavis.edu).

### ORCID

Lizhi Tao: 0000-0001-9921-2297

James C. Fettinger: 0000-0002-6428-4909

R. David Britt: 0000-0003-0889-8436

Philip P. Power: 0000-0002-6262-3209

### Notes

The authors declare no competing financial interest.

## ACKNOWLEDGMENTS

The authors thank the National Science Foundation (Grants CHE-1565501 to P.P.P. and CHE-1665455 to R.D.B.) and the Sloan Minority Ph.D. Program (CLF) for supporting this work. The authors are grateful to Peter Klavins for his supervision of the magnetic data collection.

## REFERENCES

- (a) Figgis, B. N. *Introduction to ligand fields*; Interscience Publishers, 1966. (b) van der Vlugt, J. I. Cooperative Catalysis with First-Row Late Transition Metals. *Eur. J. Inorg. Chem.* **2012**, 2012, 363–375.
- (a) Power, P. P. Stable Two-coordinate, Open-shell (d<sup>1</sup>–d<sup>9</sup>) Transition Metal Complexes. *Chem. Rev.* **2012**, 112, 3482–3507. (b) Bunting, P. C.; Atanasov, M.; Damgaard-Møller, E.; Perfetti, M.; Crassee, I.; Orlita, M.; Overgaard, J.; van Slageren, J.; Neese, F.; Long, J. R. A Linear Cobalt (II) Complex with Maximal Orbital Angular Momentum from a non-Aufbau Ground State. *Science* **2018**, 362, eaat7319. (c) Du, J.; Wang, L.; Xie, M.; Deng, L. A Two-Coordinate

Cobalt (II) Imido Complex with NHC Ligation: Synthesis, Structure, and Reactivity. *Angew. Chem., Int. Ed.* **2015**, *54*, 12640–12644. (d) Lipschutz, M. I.; Yang, X.; Chatterjee, R.; Tilley, T. D. A Structurally Rigid Bis(amido) Ligand Framework in Low-Coordinate Ni(I), Ni(II), and Ni(III) Analogues Provides Access to a Ni(III) Methyl Complex via Oxidative Addition. *J. Am. Chem. Soc.* **2013**, *135*, 15298–15301. (e) Cai, I. C.; Lipschutz, M. I.; Tilley, T. D. A bis (amido) ligand set that supports two-coordinate chromium in the +1, +2, and +3 oxidation states. *Chem. Commun.* **2014**, *50*, 13062–13065. (f) Boynton, J. N.; Guo, J.-D.; Fettinger, J. C.; Melton, C. E.; Nagase, S.; Power, P. P. Linear and Nonlinear Two-Coordinate Vanadium Complexes: Synthesis, Characterization, and Magnetic Properties of V (II) Amides. *J. Am. Chem. Soc.* **2013**, *135*, 10720–10728. (g) Zadrozy, J. M.; Atanasov, M.; Bryan, A. M.; Lin, C.-Y.; Rekken, B. D.; Power, P. P.; Neese, F.; Long, J. R. Slow magnetization dynamics in a series of two-coordinate iron (II) complexes. *Chem. Sci.* **2013**, *4*, 125–138. (h) Lin, C.-Y.; Fettinger, J. C.; Grandjean, F.; Long, G. J.; Power, P. P. Synthesis, Structure, and Magnetic and Electrochemical Properties of Quasi-Linear and Linear Iron(I), Cobalt(I), and Nickel(I) Amido Complexes. *Inorg. Chem.* **2014**, *53*, 9400–9406. (i) Lappert, M.; Protchenko, A.; Power, P.; Seeber, A. *Metal amide chemistry*; John Wiley & Sons, 2008. (j) Lappert, M.; Power, P.; Sanger, A.; Srivastava, R. *Metal and Metalloid Amides: Synthesis, Physical Properties and Structures*; Ellis, Horwood-Wiley: New York, 1980.

(3) (a) Sharpe, H. R.; Geer, A. M.; Taylor, L. J.; Gridley, B. M.; Blundell, T. J.; Blake, A. J.; Davies, E. S.; Lewis, W.; McMaster, J.; Robinson, D.; Kays, D. L. Selective reduction and homologation of carbon monoxide by organometallic iron complexes. *Nat. Commun.* **2018**, *9*, 3757. (b) Sharpe, H. R.; Geer, A. M.; Blundell, T. J.; Hastings, F. R.; Fay, M. W.; Rance, G. A.; Lewis, W.; Blake, A. J.; Kays, D. L. Dehydrocoupling of dimethylamine-borane promoted by manganese(II) m-terphenyl complexes. *Catal. Sci. Technol.* **2018**, *8*, 229–235. (c) Zadrozy, J. M.; Xiao, D. J.; Atanasov, M.; Long, G. J.; Grandjean, F.; Neese, F.; Long, J. R. Magnetic blocking in a linear iron (I) complex. *Nat. Chem.* **2013**, *5*, 577.

(4) (a) Buttrus, N. H.; Eaborn, C.; Hitchcock, P. B.; Smith, J. D.; Sullivan, A. C. Preparation and crystal structure of a two-co-ordinate manganese compound, bis[tris(trimethylsilylmethyl) manganese. *J. Chem. Soc., Chem. Commun.* **1985**, 1380–1381. (b) Viehhaus, T.; Schwarz, W.; Hübner, K.; Locke, K.; Weidlein, J. Das unterschiedliche Reaktionsverhalten von basefreiem Tris (trimethylsilyl) methyl-Lithium gegenüber den Trihalogeniden der Erdmetalle und des Eisens. *Z. Anorg. Allg. Chem.* **2001**, *627*, 715–725. (c) Merrill, W. A.; Stich, T. A.; Brynda, M.; Yeagle, G. J.; Fettinger, J. C.; De Hont, R.; Reiff, W. M.; Schulz, C. E.; Britt, R. D.; Power, P. P. Direct Spectroscopic Observation of Large Quenching of First-Order Orbital Angular Momentum with Bending in Monomeric, Two-Coordinate Fe(II) Primary Amido Complexes and the Profound Magnetic Effects of the Absence of Jahn- and Renner-Teller Distortions in Rigorously Linear Coordination. *J. Am. Chem. Soc.* **2009**, *131*, 12693–12702. (d) Bryan, A. M.; Merrill, W. A.; Reiff, W. M.; Fettinger, J. C.; Power, P. P. Synthesis, Structural, and Magnetic Characterization of Linear and Bent Geometry Cobalt (II) and Nickel (II) Amido Complexes: Evidence of Very Large Spin-Orbit Coupling Effects in Rigorously Linear Coordinated Co<sup>2+</sup>. *Inorg. Chem.* **2012**, *51*, 3366–3373. (e) Chen, H.; Bartlett, R. A.; Olmstead, M. M.; Power, P. P.; Shoner, S. C. Series of two-coordinate and quasi-two-coordinate transition-metal complexes: synthesis, structural, and spectroscopic studies of sterically demanding borylamide ligands -NRBR'<sub>2</sub> (R = Ph, R' = Mes, Xyl; R = R' = Mes), their lithium salts, Li(Et<sub>2</sub>O)<sub>2</sub>NRBR'<sub>2</sub>, and their transition-metal derivatives, M(NPhBMes)<sub>2</sub> (M = Cr, Co, Ni), Co(NPhBXyl)<sub>2</sub> and M(NMesBMes)<sub>2</sub> (M = Cr → Ni). *J. Am. Chem. Soc.* **1990**, *112*, 1048–1055. (f) Bartlett, R. A.; Feng, X.; Olmstead, M. M.; Power, P. P.; Weese, K. J. Synthesis and x-ray structural characterization of the metal borylamide complexes Li(Et<sub>2</sub>O)<sub>2</sub>NPhBMes<sub>2</sub>, (THF)(Et<sub>2</sub>O)<sub>2</sub>LiClCo{NPhBMes<sub>2</sub>}<sub>2</sub>, and Mn-{NMesBMes<sub>2</sub>}<sub>2</sub>·3PhMe (Mes = 2,4,6-Me<sub>3</sub>C<sub>6</sub>H<sub>2</sub>): modified amide ligands with poor bridging and pi-donor characteristics. *J. Am. Chem. Soc.* **1987**, *109*, 4851–4854. (g) Bartlett, R. A.; Power, P. P. Two-coordinate, nonlinear, crystalline d<sup>6</sup> and d<sup>7</sup> complexes: syntheses and structures of M{N(SiMePh<sub>2</sub>)<sub>2</sub>}, M = Fe or Co. *J. Am. Chem. Soc.* **1987**, *109*, 7563–7564. (h) Kays, D. L.; Cowley, A. R. Monomeric, two-coordinate Mn, Fe and Co(II) complexes featuring 2,6-(2,4,6-trimethylphenyl)phenyl ligands. *Chem. Commun.* **2007**, 1053–1055. (i) Ni, C.; Power, P. P. Insertion reactions of a two-coordinate iron diaryl with dioxygen and carbon monoxide. *Chem. Commun.* **2009**, 5543–5545. (j) Ni, C.; Stich, T. A.; Long, G. J.; Power, P. P. Unusual magnetic properties of a two-coordinate heteroleptic linear cobalt (II) complex. *Chem. Commun.* **2010**, *46*, 4466–4468. (k) Wehmschulte, R. J.; Power, P. P. Synthesis and Characterization of the sigma-Bonded, Quasi-Linear, Metal(II) Diaryls MMes<sub>2</sub> (M = Mg, Mn, Fe; Mes = 2,4,6-tert-Bu<sub>3</sub>C<sub>6</sub>H<sub>2</sub>). *Organometallics* **1995**, *14*, 3264–3267. (l) Mo, Z.; Chen, D.; Leng, X.; Deng, L. Intramolecular C (sp<sup>3</sup>)-H Bond Activation Reactions of Low-Valent Cobalt Complexes with Coordination Unsaturation. *Organometallics* **2012**, *31*, 7040–7043. (m) Arduengo, A. J.; Gamper, S. F.; Calabrese, J. C.; Davidson, F. Low-Coordinate Carbene Complexes of Nickel(0) and Platinum(0). *J. Am. Chem. Soc.* **1994**, *116*, 4391–4394.

(5) Lin, C.-Y.; Guo, J.-D.; Fettinger, J. C.; Nagase, S.; Grandjean, F.; Long, G. J.; Chilton, N. F.; Power, P. P. Dispersion Force Stabilized Two-Coordinate Transition Metal-Amido Complexes of the -N(SiMe<sub>3</sub>)Dipp (Dipp = C<sub>6</sub>H<sub>3</sub>-2,6-iPr<sub>2</sub>) Ligand: Structural, Spectroscopic, Magnetic, and Computational Studies. *Inorg. Chem.* **2013**, *52*, 13584–13593.

(6) (a) Werncke, C. G.; Suturina, E.; Bunting, P. C.; Vendier, L.; Long, J. R.; Atanasov, M.; Neese, F.; Sabo-Etienne, S.; Bontemps, S. Homoleptic Two-Coordinate Silylamido Complexes of Chromium (I), Manganese (I), and Cobalt (I). *Chem. - Eur. J.* **2016**, *22*, 1668–1674. (b) Lipschutz, M. I.; Tilley, T. D. Synthesis and Reactivity of a Conveniently Prepared Two-coordinate Bis(amido) Nickel (II) Complex. *Chem. Commun.* **2012**, *48*, 7146–7148. (c) Wagner, C. L.; Tao, L.; Thompson, E. J.; Stich, T. A.; Guo, J.; Fettinger, J. C.; Berben, L. A.; Britt, R. D.; Nagase, S.; Power, P. P. Dispersion-Force-Assisted Disproportionation: A Stable Two-Coordinate Copper (II) Complex. *Angew. Chem., Int. Ed.* **2016**, *55*, 10444–10447. (d) Schumann, H.; Gottfriedsen, J.; Dechert, S.; Girmsdies, F. Homoleptische Amide von Zink, Cadmium und Quecksilber. *Z. Anorg. Allg. Chem.* **2000**, *626*, 747–758.

(7) Liptrot, D. J.; Power, P. P. London dispersion forces in sterically crowded inorganic and organometallic molecules. *Nature Reviews Chemistry* **2017**, *1*, 0004.

(8) Shen, B.; Ying, L.; Chen, J.; Luo, Y. Synthesis and characterization of yttrium complexes bearing a bulky arylamido ancillary ligand. *Inorg. Chim. Acta* **2008**, *361*, 1255–1260.

(9) Haaland, A.; Hedberg, K.; Power, P. P. Molecular structure of bis [bis (trimethylsilyl) amino] zinc as determined by gas electron diffraction. *Inorg. Chem.* **1984**, *23*, 1972–1975.

(10) Margraf, G.; Lerner, H.-W.; Bolte, M.; Wagner, M. Kristallstruktur des Zinkamids Zn[N(SiMe<sub>3</sub>)<sub>2</sub>]<sub>2</sub>. *Z. Anorg. Allg. Chem.* **2004**, *630*, 217–218.

(11) Chen, H.; Bartlett, R. A.; Dias, H. V. R.; Olmstead, M. M.; Power, P. P. The use of very crowded silylamine ligands -N(SiMe<sub>n</sub>Ph<sub>3-n</sub>)<sub>2</sub> (n = 0, 1, or 2) to synthesize crystalline, two-coordinate, derivatives to manganese(II), iron(II), and cobalt(II) and the free ion [Ph<sub>3</sub>SiNSiPh<sub>3</sub>]. *J. Am. Chem. Soc.* **1989**, *111*, 4338–4345.

(12) Ashley, A. E.; Cowley, A. R.; Green, J. C.; Johnston, D. R.; Watkin, D. J.; Kays, D. L. Synthesis and Characterisation of Low-Coordinate Transition-Metal Complexes Stabilised by Sterically Demanding Carbazolido Ligands. *Eur. J. Inorg. Chem.* **2009**, *2009*, 2547–2552.

(13) Au-Yeung, H. Y.; Lam, C. H.; Lam, C.-K.; Wong, W.-Y.; Lee, H. K. Unusual Iron(II) and Cobalt(II) Complexes Derived from Monodentate Arylamido Ligands. *Inorg. Chem.* **2007**, *46*, 7695–7697.

(14) Reiff, W. M.; Schulz, C. E.; Whangbo, M.-H.; Seo, J. I.; Lee, Y. S.; Potratz, G. R.; Spicer, C. W.; Girolami, G. S. Consequences of a Linear Two-Coordinate Geometry for the Orbital Magnetism and

Jahn-Teller Distortion Behavior of the High Spin Iron(II) Complex  $\text{Fe}[\text{N}(\text{t-Bu})_2]_2$ . *J. Am. Chem. Soc.* **2009**, *131*, 404–405.

(15) Figgis, B. N.; Lewis, J.; Mabbs, F. E.; Webb, G. A. The magnetic behaviour of cubic field  $^5\text{T}_2$  terms in lower symmetry. *J. Chem. Soc. A* **1967**, 442–447.

(16) Reiff, W. M.; LaPointe, A. M.; Witten, E. H. Virtual Free Ion Magnetism and the Absence of Jahn-Teller Distortion in a Linear Two-Coordinate Complex of High-Spin Iron(II). *J. Am. Chem. Soc.* **2004**, *126*, 10206–10207.

(17) Meng, Y.-S.; Mo, Z.; Wang, B.-W.; Zhang, Y.-Q.; Deng, L.; Gao, S. Observation of the single-ion magnet behavior of  $\text{d}^8$  ions on two-coordinate Co (I)-NHC complexes. *Chem. Sci.* **2015**, *6*, 7156–7162.

(18) Nguyen, T.; Panda, A.; Olmstead, M. M.; Richards, A. F.; Stender, M.; Brynda, M.; Power, P. P. Synthesis and Characterization of Quasi-Two-Coordinate Transition Metal Dithiolates  $\text{M}(\text{SAr}^*)_2$  ( $\text{M} = \text{Cr}, \text{Mn}, \text{Fe}, \text{Co}, \text{Ni}, \text{Zn}; \text{Ar}^* = \text{C}_6\text{H}_5\text{-}2, 6(\text{C}_6\text{H}_2\text{-}2,4,6\text{-iPr}_3)_2$ ). *J. Am. Chem. Soc.* **2005**, *127*, 8545–8552.

(19) Bryan, A. M.; Merrill, W. A.; Reiff, W. M.; Fettinger, J. C.; Power, P. P. Synthesis, Structural, and Magnetic Characterization of Linear and Bent Geometry Cobalt(II) and Nickel(II) Amido Complexes: Evidence of Very Large Spin-Orbit Coupling Effects in Rigorously Linear Coordinated  $\text{Co}^{2+}$ . *Inorg. Chem.* **2012**, *51*, 3366–3373.

(20) (a) Bellow, J. A.; Yousif, M.; Fang, D.; Kratz, E. G.; Cisneros, G. A.; Groysman, S. Synthesis and Reactions of 3d Metal Complexes with the Bulky Alkoxide Ligand  $[\text{OCtBu}_2\text{Ph}]$ . *Inorg. Chem.* **2015**, *54*, 5624–5633. (b) Purdy, A. P.; George, C. F. Volatile copper and barium-copper alkoxides. Crystal structure of a tricoordinate copper(II) complex,  $\text{Ba}(\text{Cu}[\text{OCMe}(\text{CF}_3)_2])_3$ . *Inorg. Chem.* **1991**, *30*, 1969–1970. (c) Stibraný, R. T.; Zhang, C.; Emge, T. J.; Schugar, H. J.; Potenza, J. A.; Knapp, S. A. Tris(pyrazolyl)  $\eta^6$ -Arene Ligand That Selects Cu(I) over Cu(II). *Inorg. Chem.* **2006**, *45*, 9713–9720. (d) Sorrell, T. N.; Jameson, D. L. Synthesis and characterization of sterically hindered  $\text{CuN}_4$  complexes of tripod ligands. *Inorg. Chem.* **1982**, *21*, 1014–1019. (e) Schröter-Schmid, I.; Strähle, J. Synthese und Struktur von Thiolatokomplexen des einwertigen Kupfers: Tetrameres und Octameres  $[\text{CuSC}_6\text{H}_2(\text{i-Pr})_3]$ . Synthesis and Structure of Thiolato Complexes of Monovalent Copper: Tetrameric and Octameric  $[\text{CuSC}_6\text{H}_2(\text{i-Pr})_3]$ . *Z. Naturforsch., B: J. Chem. Sci.* **1990**, *45*, 1537. (f) Becker, B.; Wojnowski, W.; Peters, K.; Peters, E.-M.; Von Schnering, H. G. Contributions to the chemistry of silicon-sulphur compounds—LXVII. Synthesis, molecular structure and properties of cyclo-tetrakis-[tri-tert-butoxysilanethiolatocopper(I)],  $[(\text{t-C}_4\text{H}_9\text{O})_3\text{SiSCu}]_4$ , the first example of a square planar  $\text{Cu}_4\text{S}_4$  ring. *Polyhedron* **1990**, *9*, 1659–1666. (g) James, A. M.; Laxman, R. K.; Fronczek, F. R.; Maverick, A. W. Phosphorescence and Structure of a Tetrameric Copper(I)-Amide Cluster. *Inorg. Chem.* **1998**, *37*, 3785–3791.

(21) Cai, I. C.; Ziegler, M. S.; Bunting, P. C.; Nicolay, A.; Levine, D. S.; Kalendra, V.; Smith, P. W.; Lakshmi, K. V.; Tilley, T. D. Monomeric, Divalent Vanadium Bis(arylamido) Complexes: Linkage Isomerism and Reactivity. *Organometallics* **2019**, *38*, 1648–1663.

(22) Bakhoda, A.; Jiang, Q.; Bertke, J. A.; Cundari, T. R.; Warren, T. H. Elusive Terminal Copper Arylnitrene Intermediates. *Angew. Chem., Int. Ed.* **2017**, *56*, 6426–6430.

(23) Hu, G.; Holmes, D.; Gendhar, B. F.; Wulff, W. D. Optically Active (aR)- and (aS)-Linear and Vaulted Biaryl Ligands: Deracemization versus Oxidative Dimerization. *J. Am. Chem. Soc.* **2009**, *131*, 14355–14364.

(24) (a) Chen, H.; Olmstead, M. M.; Shoner, S. C.; Power, P. P. Tri- and tetra-meric copper (I) amides  $\{\text{Cu}[\text{N}(\text{SiMe}_2\text{Ph})_2]\}_3$  and  $\{\text{Cu}[\text{N}(\text{SiMe}_2\text{Ph})_2]\}_4$ . *J. Chem. Soc., Dalton Trans.* **1992**, 451–457. (b) Eaborn, C.; Hitchcock, P. B.; Smith, J. D.; Sullivan, A. C. Preparation and crystal structure of the tetrahydrofuran adduct of lithium bis [tris(trimethylsilyl)methyl]cuprate,  $[\text{Li}(\text{THF})_4][\text{Cu}\{\text{C}(\text{SiMe}_3)_2\}_2]$ . The first structural characterization of a Gilman reagent. *J. Organomet. Chem.* **1984**, *263*, c23–c25.

(25) Tang, Y.; Zakharov, L. N.; Rheingold, A. L.; Kemp, R. A. Two new bulky amido ligands useful for the preparation of metal complexes and examples of their reactivity. *Inorg. Chim. Acta* **2006**, *359*, 775–781.